



5-2017

Enceladus Sample Return Mission

Braxton Brakefield

University of Tennessee, Knoxville, bbrakefi@vols.utk.edu

Rekesh Ali

University of Tennessee, Knoxville, rali1@vols.utk.edu

Andrew Bishop

University of Tennessee, Knoxville, abishop9@vols.utk.edu

Shelby Honaker

University of Tennessee, Knoxville, shonaker@vols.utk.edu

David Taylor

University of Tennessee, Knoxville, dtaylo45@vols.utk.edu

Follow this and additional works at: https://trace.tennessee.edu/utk_chanhonoproj

 Part of the [Aerodynamics and Fluid Mechanics Commons](#), [Astrodynamics Commons](#), [Space Vehicles Commons](#), and the [Systems Engineering and Multidisciplinary Design Optimization Commons](#)

Recommended Citation

Brakefield, Braxton; Ali, Rekesh; Bishop, Andrew; Honaker, Shelby; and Taylor, David, "Enceladus Sample Return Mission" (2017).

University of Tennessee Honors Thesis Projects.

https://trace.tennessee.edu/utk_chanhonoproj/2109

This Dissertation/Thesis is brought to you for free and open access by the University of Tennessee Honors Program at Trace: Tennessee Research and Creative Exchange. It has been accepted for inclusion in University of Tennessee Honors Thesis Projects by an authorized administrator of Trace: Tennessee Research and Creative Exchange. For more information, please contact trace@utk.edu.

ENCELADUS SAMPLE RETURN MISSION

Rekesh M. Ali,^{*} Andrew S. Bishop,[†] Braxton Brakefield,[‡] Shelby Honaker,[§]
Brier Taylor^{**} and James E. Lyne^{††}

The Cassini mission has confirmed that Enceladus has a subsurface liquid ocean and hydrothermal vents that may support life, as well as geysers that eject water from beneath the frozen surface into space. This provides an unusual opportunity to sample the interior without necessitating a landing. In this study, a novel, flyby sample return mission is examined, using a previously published free-return interplanetary trajectory. We propose the use of multiple small pods that would be released from a carrier bus prior to the Enceladus encounter. These pods would collect ejected material during flyby and would each return to Earth independently, thereby reducing or eliminating the possibility of a single point failure after the pod release. The pods would enter Earth's atmosphere at a speed of 15.7 km/s, by far the fastest Earth entry to date. The small size of the pods tends to reduce their ballistic coefficient, thereby making such a high entry speed potentially feasible.

INTRODUCTION

This current work is an extension of previous research carried out at the University of Tennessee on high speed atmospheric entry, free-return interplanetary trajectories, and novel Enceladus mission concepts.¹⁻⁴ The proposed scenario takes advantage of the known geysers on Enceladus to enable a sample return without the need for orbital capture or landing. The geysers on Enceladus eject many kilograms per second of material into the space around Saturn, likely being responsible for the existence of the planet's E-ring. The composition of the material ejected from these geysers could yield valuable information about the conditions of, and whether or not there is, life within the oceans beneath the frozen crust of Enceladus.

The design iterations for this mission include testing flybys of Venus, Earth, and Jupiter to determine the most efficient trajectory possible. Program to Optimize Simulated Trajectories (POST) and Mission Analysis Environment (MAnE) simulations are presented, showing the trajectories approaching Saturn and re-entering Earth's atmosphere, respectively. These simulations account for the shape, mass, and size of the probes, along with the dimensions and properties of

^{*} Student, M.A.B.E. department, University of Tennessee, Knoxville, 1512 Middle Drive, Knoxville, TN 37996-2210.

[†] Student, M.A.B.E. department, University of Tennessee, Knoxville, 1512 Middle Drive, Knoxville, TN 37996-2210.

[‡] Student, M.A.B.E. department, University of Tennessee, Knoxville, 1512 Middle Drive, Knoxville, TN 37996-2210.

[§] Student, M.A.B.E. department, University of Tennessee, Knoxville, 1512 Middle Drive, Knoxville, TN 37996-2210.

^{**} Student, M.A.B.E. department, University of Tennessee, Knoxville, 1512 Middle Drive, Knoxville, TN 37996-2210.

^{††} Clinical Associate Professor, M.A.B.E. department, University of Tennessee, Knoxville, 1512 Middle Drive, 062 Perkins Hall, Knoxville, TN 37996-2210.

the necessary thermal protective system (TPS). To ensure the methodology, a Stardust re-entry replication is corroborated with NASA's figures describing the actual Stardust's descent.

The chosen deep space trajectory, from the research conducted by Jones⁵, is approximately twenty-five years in duration with a launch date July 27th, 2025. The bus is projected to approach Saturn at 8 km/s and return to Earth going 15.7 km/s, which is about 25% more than Stardust—the fastest entry to date. The unprecedented nature of this high-speed entry poses certain problems: identifying a body size and shape, in conjunction with entry angle, to minimize total heat load, choosing a durable ablative heat shield, and selecting a set of lightweight but dependable parachute systems. Small, Stardust shaped bodies at high angles of attack do well to keep the heat load down. Stardust's Phenolic Impregnated Carbon Ablator (PICA) is chosen for the TPS due to its light weight and resistance against higher dynamic pressures. For a first pass analysis, the smallness of the return capsules nullifies parachute complications, because of their velocities at altitudes like Stardust's deployment levels.

METHODOLOGY

MAAnE

Mission Analysis Environment, MAAnE, is a software commonly used to create trajectories for missions inside of the solar system. Originally, the mission plan was to create trajectories using multiple Earth, Venus, and Jupiter flybys such that a free return path from Saturn could be utilized with minimal C3 values. Many problems arose, such as finding a reasonable launch date and minimizing mission times. These issues prompted research into previously organized relevant trajectories, most notably those within Jones' paper on possible Saturn free return missions⁵. A route that Jones discovered is re-simulated with MAAnE to generate a more detailed mission timeline to identify key long-term trajectory elements.

POST

The Program to Optimize Simulated Trajectories (POST) is a software designed by NASA that can simulate any object passing through a user defined atmosphere. For this design, POST is used to model the re-entry of the probes once they return to Earth. As these probes are re-entering at speeds much faster than seen in any other missions, approximately 16 km/s, surviving the thick atmosphere of Earth is one of the greater challenges facing this proposal.

No one on the team had used POST prior to conducting this research, which necessitates validation in some way so that accuracy is ensured. For this, the entry conditions⁶, aerodynamics⁷, and physical parameters⁸ of Stardust are required for a POST re-simulation of its descent. The resulting output is to be compared to the actual performance of the Stardust re-entry capsule. The choice of using Stardust for validation rather than Hayabusa⁹ stems from the quantity of relevant information available for either capsule, including entry location, ground track, and descent speeds, among others.

Following validation, a multitude of POST runs are compared to identify what a favorable design of the re-entry capsules may look like. Diameters ranging from 10 cm to 100 cm are tested, with weights scaled to both Stardust and Hayabusa. The aerodynamics of a hemisphere, the Stardust re-entry probe, and the Hayabusa re-entry probe all undergo testing to establish a preferred shape. The entry angle is varied between 5 and 45 degrees to determine the effects of initial orientation. For completeness, free molecular and transition regime aerodynamics should be included to indicate changes in descent due to relatively large Knudsen Numbers.

HEATING

Convective

Convective heating rate is initially calculated using the analytical relationship from Marvin and Deiwert¹⁰. However, some values for the equation, such as enthalpy ratio, are difficult to be determined, and so are replaced with very rough estimations. The lackluster implementation of this method prompts desire for a better estimation. Apparently, POST is capable of outputting convective heating rates along the capsule's descent, so it is the currently preferred method.

Radiative

The analytical methods of Tauber and Sutton¹¹ are used in the first wave of radiative heating calculations. Unfortunately, these solutions are accompanied by strict body size limitations, which ostracize some necessary runs. Luckily, in-house radiative heating for small bodies has been researched in quite the excess, and documents are available on hand. Jakob Brisby's dissertation¹² involves a hyper in-depth curve fit of the numbers tabulated by Sutton and Hartung¹³. This curve fit has more forgiving body size limits, so it is employed to more accurately calculate the probe heating data.

PROBE DESIGN

Aerodynamics

In the first phase of this design, re-entry return capsules were strictly spherical in shape, so that methodology could be properly practiced. Now, the descent of the probe is controlled with the aerodynamics of the Stardust or Hayabusa return capsule. This decision is in effort to minimize research regarding bodies in high speed flow, as both shapes have an already proven performance ability. For a first pass, the bodies are scaled into a smaller size with their respective densities at nominal values. A diagram of Stardust is shown in Figure 1.

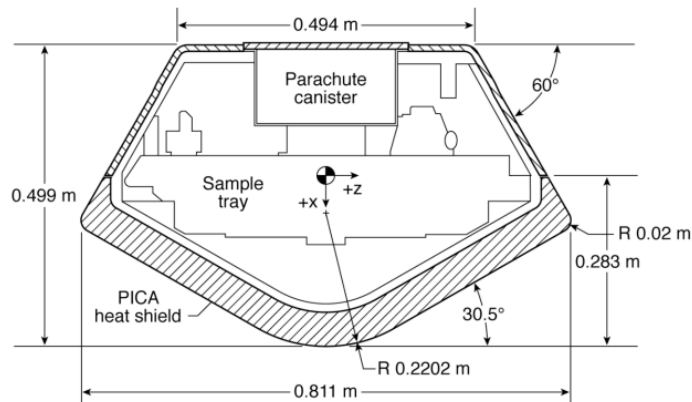


Figure 1: Diagram of the Stardust Entry Capsule

Collection

Aerogel is chosen as the main material to capture the geyser particles due to its low density and reliable design. Aerogel's specific material properties can be observed in Appendix A. In addition, Stardust employed a "tennis racket" design that this capture system will also use. The fore body heat shield hinges open and the racket extrudes for collection. The particles lodge them-

selves into the aerogel and are effectively preserved inside of the material so that there is minimal decomposition during the return voyage. The "tennis racket" device is shown in Figure 2.

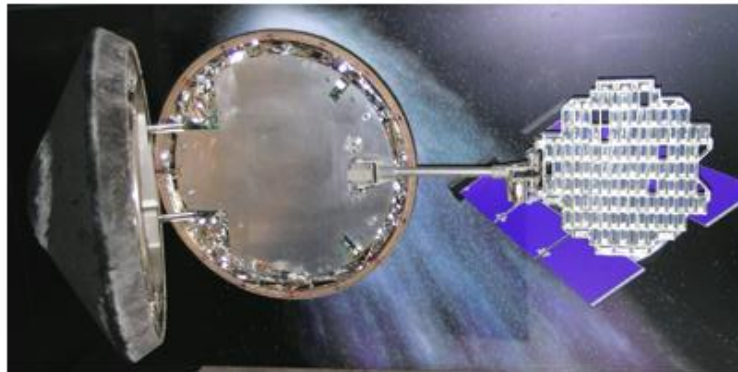


Figure 2: Stardust Material Capture System

Heat Shield

Estimation of the heat shield thickness is conducted using a linear scaling approximation with respect to Stardust's nominal thickness, recession amounts, and integrated heat load. All the specifications on Stardust's heat shield are from the McNamara, et al.¹⁴ research paper on X-ray imaging of the Stardust heat shield before and after Earth atmospheric entry. The heat shield on Stardust is PICA, therefore the estimation method only holds if the chosen heat shield is PICA. However, PICA is a great choice anyway due to the material's extremely high heat and pressure tolerances. Tran's¹⁵ paper on PICA and other ablative heat shield materials is referenced to determine the limitations and properties of the anticipated heat shield material.

Parachute

A numerical trajectory code, written in Matlab, models the deployment of both a drogue and a main parachute. Densities and temperatures are pulled from the U.S. Standard Atmosphere. The initial parachute system is chosen by analyzing both Stardust¹⁶ and Hayabusa's systems. The aerodynamics in use are for a disk-gap-band drogue and a ribbon type main chute. Area sizing is required to reasonably accommodate the scaled shapes. Parachute mass is scaled with area and deployment Mach numbers are manually tweaked until a balance between dynamic pressure and ground velocity is reached.

VALIDATION

Post

The first POST validation is presented below in Figure 3. Desai's best estimated trajectory is a post entry reconstruction of Stardust's return capsule. Initially, this presented an issue because most sources discuss only the predicted parameters of Stardust's re-entry. However, the POST simulation uses the exact entry conditions as its counterpart, and the results agree outstandingly. The maximum deviation occurs when the craft slows down the most, but the curves re-align at lower altitudes.

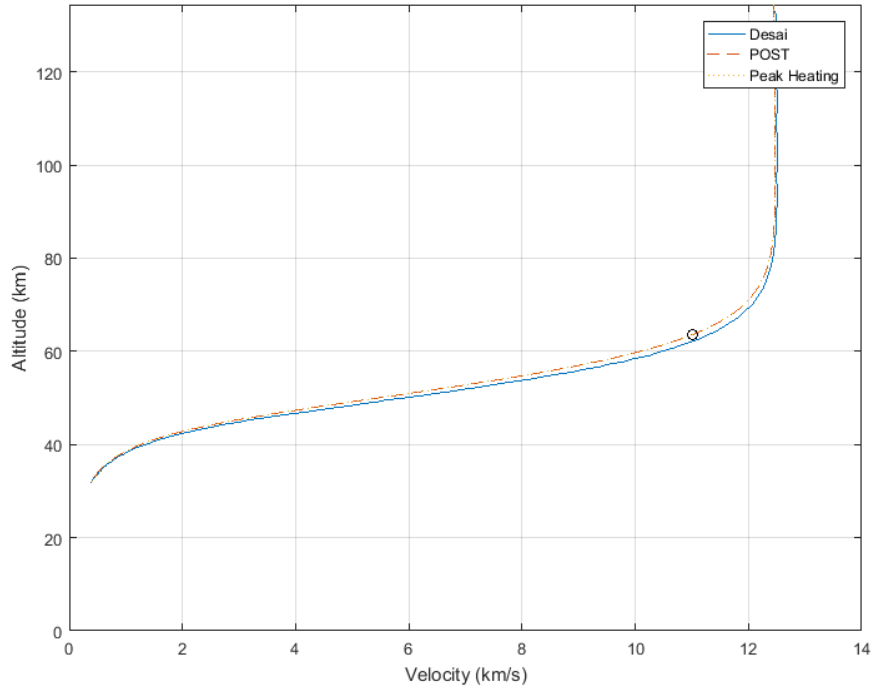


Figure 3: POST Validation Against Desai's Reconstruction, Altitude Versus Velocity

Figure 4 shows how well the POST simulation compares to the radar ground track data¹⁷ from the actual re-entry. The curves are sufficiently similar, and all questions regarding POST validation are cleared. Not only do these curves confirm the fidelity of POST simulations, it also proves that the team can use the software with high proficiency.

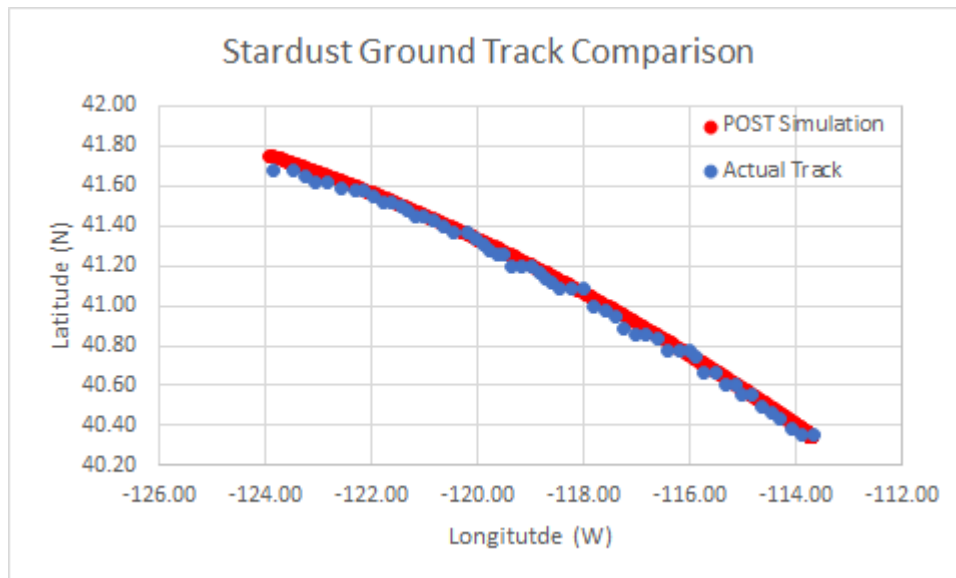


Figure 4: Stardust Simulated Versus Actual Ground Track

Heating

The mixed heating method is validated in Figure 5. Convective heating comes from POST, and radiative heating is computed at each point in the descent using Brisby's Fortran written curve fit. The heating is compared to a splicing of Kontinos' ¹⁸ and Desai's data, where Kontinos provides the heat rate, and Desai the trajectory. The curves match very well and it is clear that these methods will prove accurate when analyzing scale models.

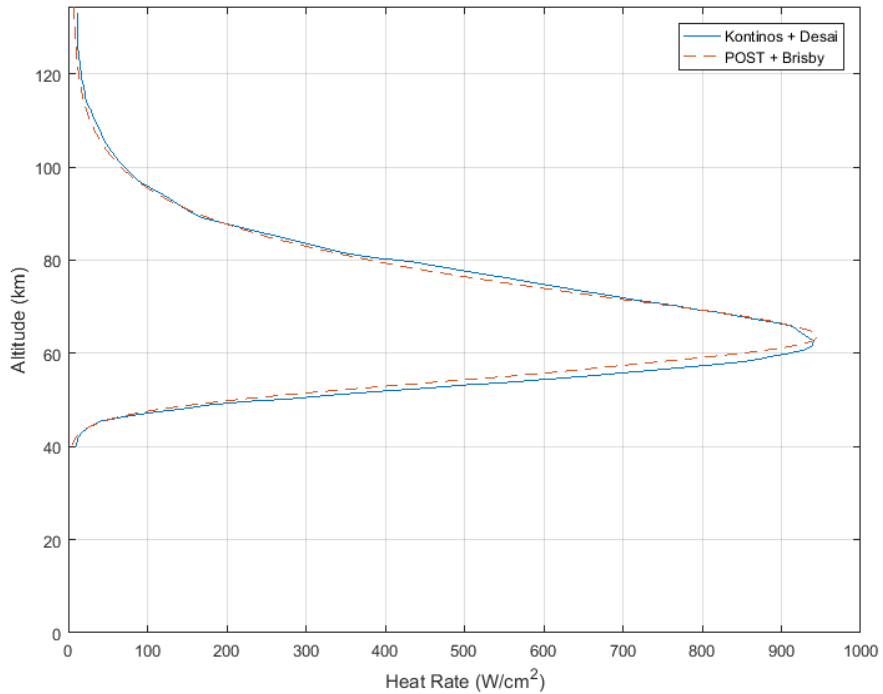


Figure 5: POST/Brisby Cross Validation with Kontinos/Desai, Altitude Versus Heat Rate

RESULTS

MAnE

A re-construction of Jones' trajectory is presented in Figure 6. The future launch and return dates using this trajectory are July 27th, 2025 at 2 a.m. EST and September 18th, 2050. The bus will approach Saturn at a hyperbolic excess speed of 8 km/s, and return to low Earth space at nearly 16 km/s, a record-breaking feat. The reason this mission duration time and the return speed are so high is because the spacecraft flies beyond the orbit of Saturn. The probes are redirected to Earth only after receiving a gravity assist. The turn angle is vast, and it sends the probes on another leg beyond the orbit of Saturn before returning to Earth. These patterns are the consequences of a free return trajectory.

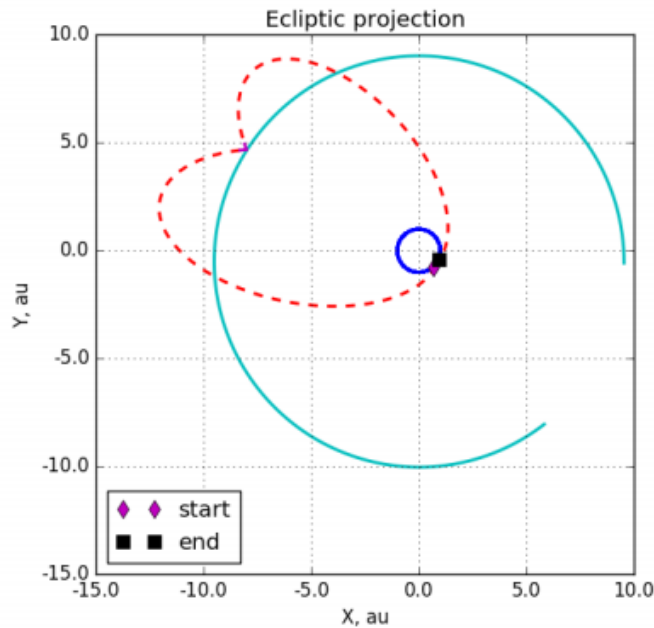


Figure 6: Free Return Trajectory Between Earth and Saturn Orbits

Post

To start, the effects of free molecular aerodynamics are investigated because the Knudsen numbers of the probes are very large at high altitudes. The combination chosen is Stardust's body scaled to 10 cm in diameter. The results are displayed in Figures 7, which show that the free molecular regime has a minimal effect on the trajectory of the probes. Due to the negligible differences, free molecular flow will be left out in the subsequent analyses.

Figure 8 illustrates how the probes slow down as they descend deeper into Earth's atmosphere. The dashed trajectory represents a Stardust replication, and the dotted lines circumscribe the window where the radiative heating calculations are conducted. The only deviations occur within 40 and 100 km, where the capsules go through the highest levels of heating. Steeper entry angles seem to keep the pods from slowing down until lower altitudes. Although they come in much faster, all of the scale models slow down at higher altitudes than Stardust's capsule. It also appears that the steeper entry angles inhibit peak heating until lower altitudes, but the peak value happens at very similar velocities for each probe. Because Stardust enters much slower, it peaks at a lower velocity. Regardless of size, all probes seem to begin peaking right when the velocity differential is increasing. The sudden thickening of the atmosphere here affects all the re-entry vehicles greatly, as it is a major factor in the trajectory patterns. At altitudes below 40 km, the curves become indistinguishable. This trend implies that a single parachute analysis for a given size may be applicable over a wide array of entry angles.

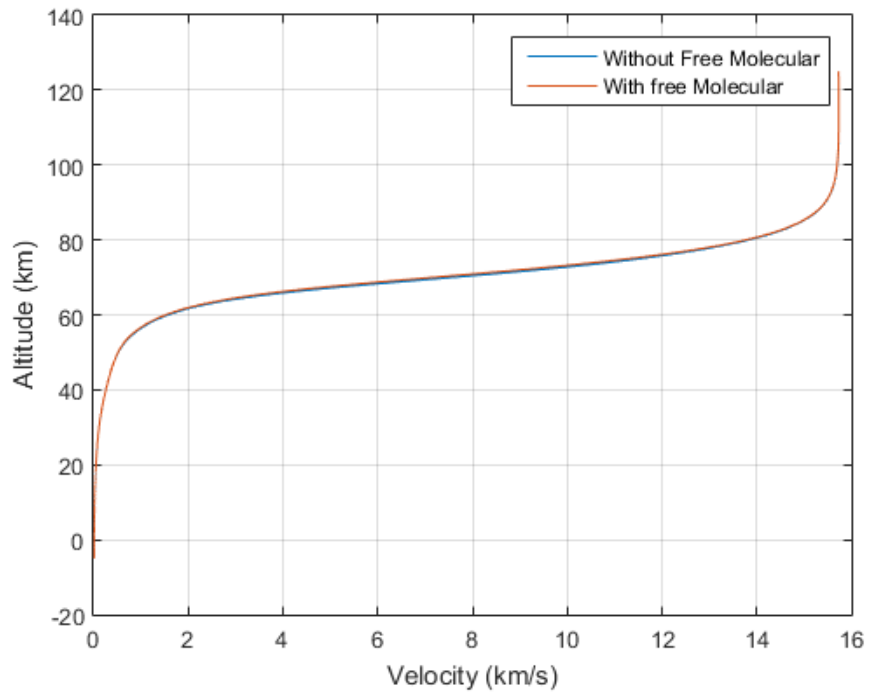


Figure 7: Comparison With and Without Free Molecular Regime Aerodynamics for a 10cm Diameter Body

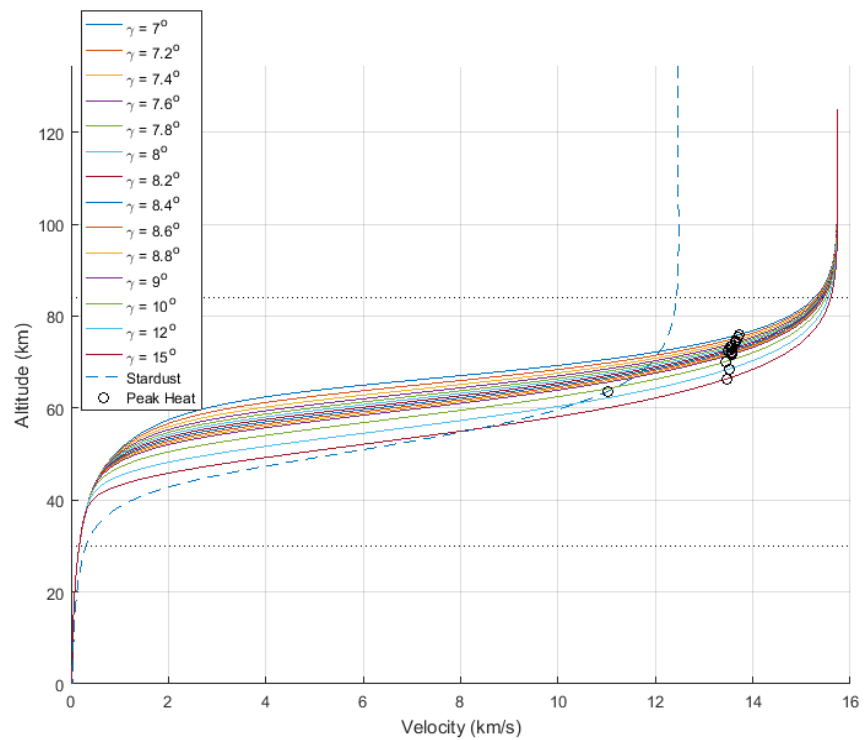


Figure 8: Altitude Versus Velocity for Stardust Scaled to a 20 cm Diameter

Heating

Figure 9 illustrates the heating rate as a 20 cm diameter probe approaches the surface of Earth. Steeper entry angles stretch the heat curve for a given body size. All probes exceed the heating of Stardust's return capsule. The integrated heat loads for a range of entry angles and bodies are given in Figure 10. The heat load is larger for higher density bodies. Wider bodies of like density also experience more total heat. Although the heat rate is higher for steeper entries, the total heat load is lower. It is promising that some probes are heated less than Stardust.

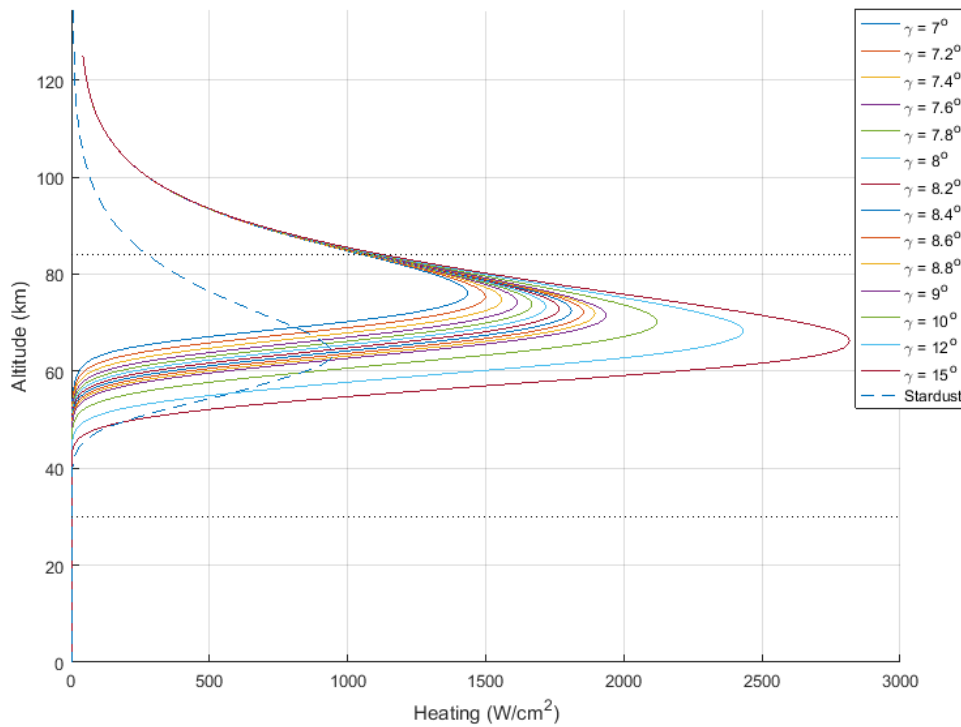


Figure 9: Altitude Versus Heating Rate for a 20cm Probe at Given Entry Angles

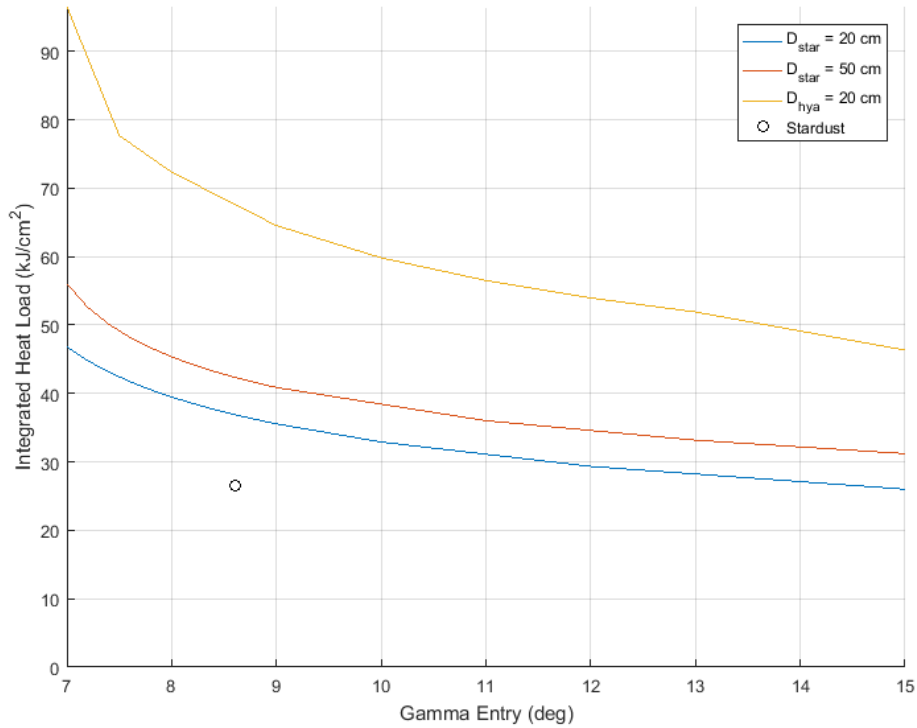


Figure 10: Integrated Heat Load for Stardust and Hayabusa Densities and Shapes at Scaled Diameters

The lower total heat loads will mean less recession amounts, thus smaller heat shields and less mass. However, the caveat is that the steeper entries suffer significantly higher stagnation dynamic pressures. With PICA being the most likely heat shield material candidate, dynamic pressure limitations are not the main concern. The structural integrity of any probes below a twenty centimeter diameter is questionable after analyzing the dynamic pressure and g-loads during entry. Calculations for probes smaller than 20 cm in diameter will likely be discarded to avoid failure. The dynamic pressure and g-load values with respect to altitude for varying entry angles are shown below in Figures 11 and 12. The dynamic pressure and g-load versus time are shown in the appendix.

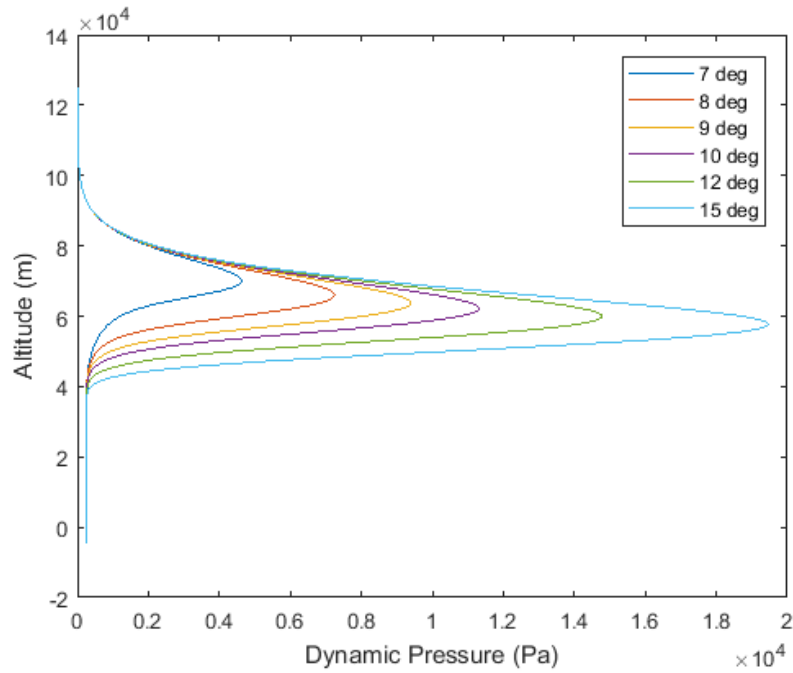


Figure 11: 20 cm Stardust Scaled Dynamic Pressure at Altitude for Varying Entry Angles

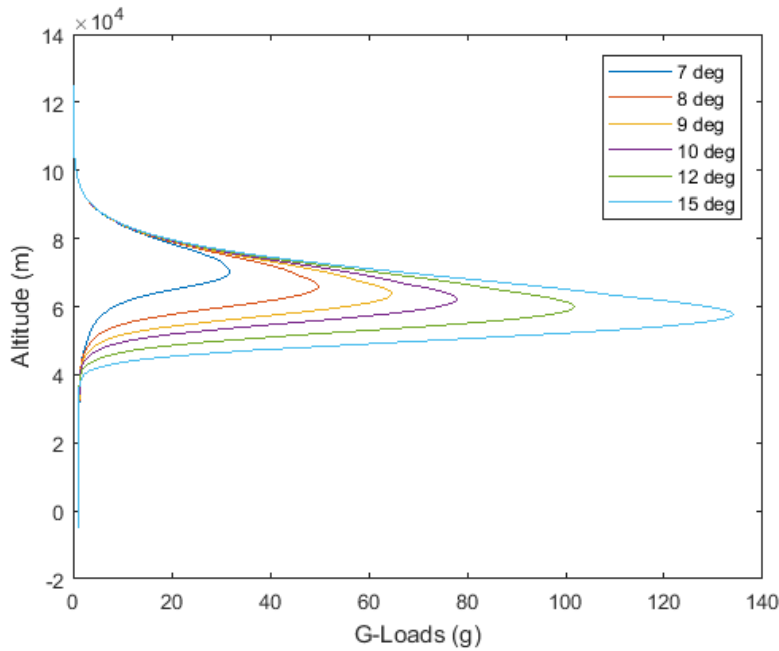


Figure 12: 20 cm Stardust Scale Acceleration at Altitude for Varying Entry Angles

Heat Shield

POST and heating data is used to calculate required heat shield thicknesses for entry angles ranging from 7 degrees to 15 degrees. Figure 13 below shows estimated recession amounts for the 20 centimeter probe, with respect to entry angle, compared to McNamara's Stardust X-rays. Figure 14 below shows the nominal heat shield thicknesses for the 20 centimeter diameter probe with

varying entry angles. These are all in comparison to the stagnation recession and side recessions of 6.3 mm and 3mm, respectively, for Stardust. Stardust's nominal heat shield thickness was 58 mm. This first pass estimate does not include any pyrolysis effects or any advanced ablation effects.

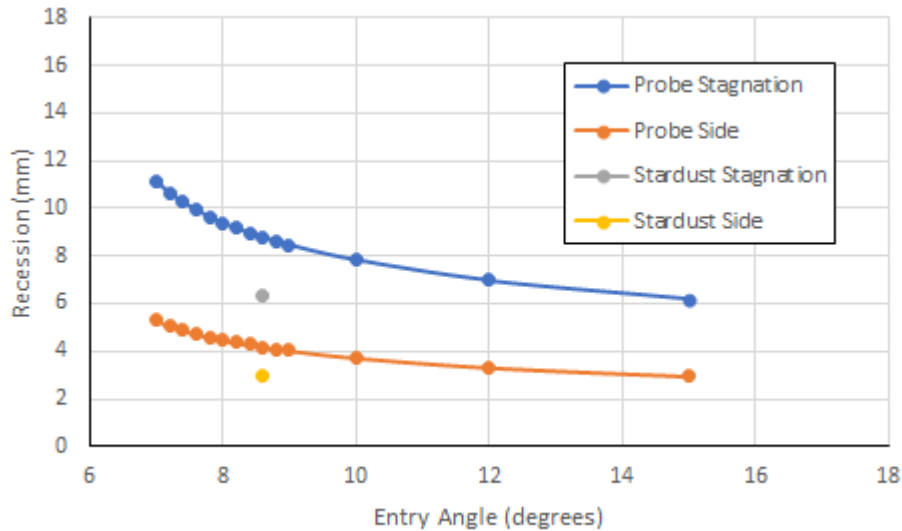


Figure 13: 20 cm Probe Heat Shield Recession Versus Entry Angle for Stardust Shape

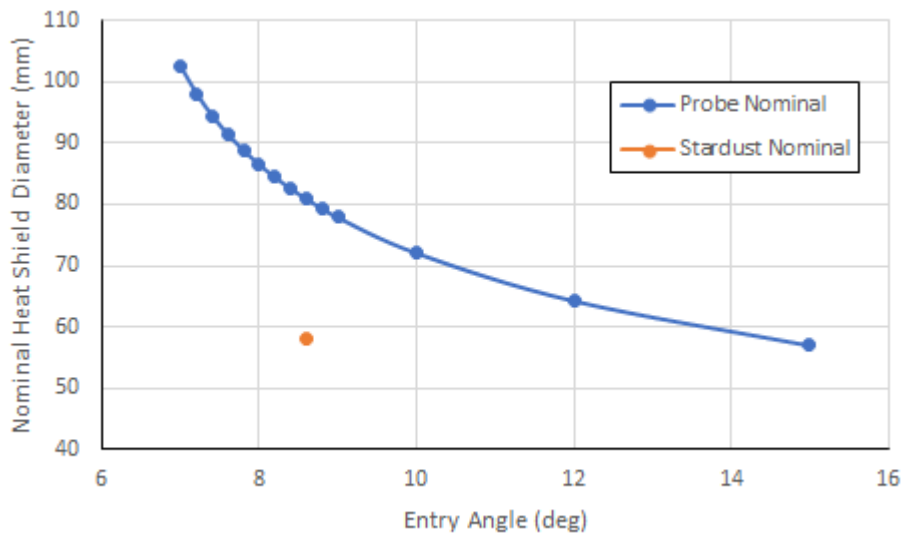


Figure 14: 20 cm Probe Nominal Heat Shield Thickness Versus Entry Angle

Parachute

Figure 15 represents a 2-dimensional modeling of the parachute deployment for a 20 cm body with a 7 degree entry angle. The simulation begins at a point long after initial re-entry, therefore the duration time does not reflect that of the full flight. The system consists of a disk-gap-band drogue parachute that is 0.5 meters in diameter. The drogue parachute deploys at Mach one, which is at an altitude of 33,000 meters. The main parachute is a ribbon chute that is 1 meter in

diameter. This parachute is deployed once the probe reaches a Mach number of 0.1, which takes place at an altitude of 15,000 meters. The capsule meets the ground at around 6 m/s. Other entry angles are omitted due to near exact similarity in results. For comparison, Stardust deployed its chutes at 32,000 meters and 2,400 meters.

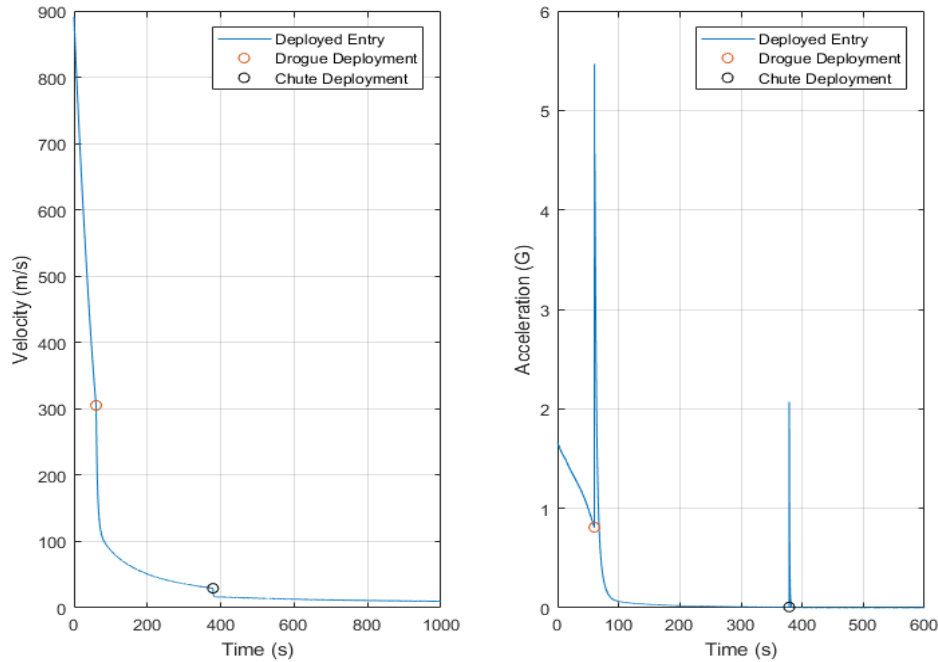


Figure 15: Parachute Deployment Simulation for 20cm Probe 7 Degree Entry

CONCLUSION

Saturn’s moon Enceladus may harbor life within the oceans beneath its thick ice layer. This proposal studies the feasibility of sending a multitude of small, pod-like, collection probes that independently return to Earth. The deep space flight path proposed by Jones offers a free return trajectory and cost effectiveness. The long duration time of the mission is a consequence of an unassisted return. Probe design investigates scale models of Stardust and Hayabusa with retained density and aerodynamics. It appears that both shapes could undergo similar heating, but the disparate results imply that density, and therefore mass, has a large role to play. This is evidenced by the more massive probes being subject to more heating, even at the same body diameter. Further studies will vary the density of each probe at regular intervals between Stardust and Hayabusa, as the current scaling method may have physical limitations. Clearly, smaller diameter probes will have less heating and more can be packed into the spacecraft, which attenuates the possibility of failure. However, the advantage to using a larger diameter includes more sample space and extra room for electronics. Although steeper entry angles lead to more severe heat rates, the integrated heat loads turn out to be much smaller than the shallow counterparts; even reaching sub-Stardust levels. This is because the higher entry angles experience appreciable heating for less time overall. The downside is that peak dynamic pressures and accelerations become increasingly large for steeper entry angles, so it may be that an entry angle between extremes is the best choice. The heat shield estimation curves are essentially a linear scale of the integrated heat load curves. Because the comparison is made with Stardust’s data, the heat shield of choice must be PICA. PICA

is an excellent choice as it can withstand higher dynamic pressures, but further analysis with industry level software would broaden the options and perhaps change this decision. The high entry velocity results in much greater peak heating than Stardust on all the probes, but more heating just means more heat shield. There may be mass concerns with this method, but Stardust only burned off about 11 % of its shield at the stagnation point, therefore it is possible these results actually indicate more than what is needed. Drogue deployment locations happen at a similar altitude to Stardust's. Main chute deployment happens much higher, and may be looked at again to address concerns regarding landing site deviations in bad weather. Dynamic pressures are not a concern at the altitudes of deployment, so deploying later would not be an issue. An analysis with higher degrees of freedom would show some insight into tumbling. Below 40 km, the altitude versus velocity graphs line up for the same size probes at different entry angles. This means that the parachute analysis for a single entry angle could feasibly be attached to different entries of the same body.

The studies for this mission confirm the possibility of successful re-entry for small scale probes returning from deep space voyages. From heating and trajectory analysis, the unprecedented entry velocity is proven tractable. This is great news for further return missions to the outer planets, especially for missions involving small-scale sample return probes. These missions may be a popular trend in the future, as the moons of some of the outer planets, such as Enceladus, could be harboring life.

ISSUES TO BE ADDRESSED

Power Systems

The power supply for the probes has yet to be determined due to the lack of available information on space battery properties. The power supply for the probes will be required to power: the aerogel mechanism used to capture Enceladus' geysers, the parachute ejection system, and a locator beacon used to find the probes after impact with Earth. Another complication is that the bus's power supply will likely be an RTG that cannot re-enter Earth's atmosphere for safety reasons. The current plan for the bus is to slightly alter the trajectory after the probe ejection to avoid Earth completely.

Advanced Ablation Effects

Pyrolysis and other advanced ablation effects were unable to be included in the initial design because of the immediate calculation difficulties without an industry standard program to assist, such as CMA or CHAR. Given a second design pass, these effects would all be included to give a significantly more accurate mass and size estimate for the heat shield on the individual probes.

Solar Power Viability

Some missions have focused on maximizing solar power usage as far away from the Sun as possible. Juno, for instance, holds the record while only generating 4% as much solar energy around Jupiter as it would if it were orbiting Earth. This poses a problem for our probes while they are trans Jupiter, but when the probes are in sub Jupiter orbit there will be plenty of potential power generation available.

On-Board Electronics

The electronics for the bus will likely include a high-resolution camera and equipment that could measure magnetic fields as the bus passes Saturn. These devices would all be commercially available and are intentionally not decided upon currently because overall mass estimations for the bus are subject to change with a second pass.

Probe Ejection System

When the bus has arrived at an optimal distance from Enceladus, the probes will be ejected to collect the geyser particulate. The method for ejecting the probes from the bus remains undecided, but the most discussed entails a minute amount of propellant intended to combust and produce a specific amount of thrust to eject the probes individually. Spring loaded launchers, such as a cubesat deployment device, were also discussed.

Solar Sails

The idea of using a solar sail on each probe to slow them down on the way back to Earth was briefly entertained during the initial planning. With a long return trip, and decreased distance to the Sun as time goes on, it was thought that a small solar sail would be effective in decreasing the return speed in order to make the re-entry less intense. However, a guidance system along with a mechanism to control the direction of thrust of the solar sail would be needed in order to ensure the probes stayed on a trajectory back to Earth. After the initial results suggested the entry would be survivable, the solar sail idea was dropped in order to keep the probes simple and reliable.

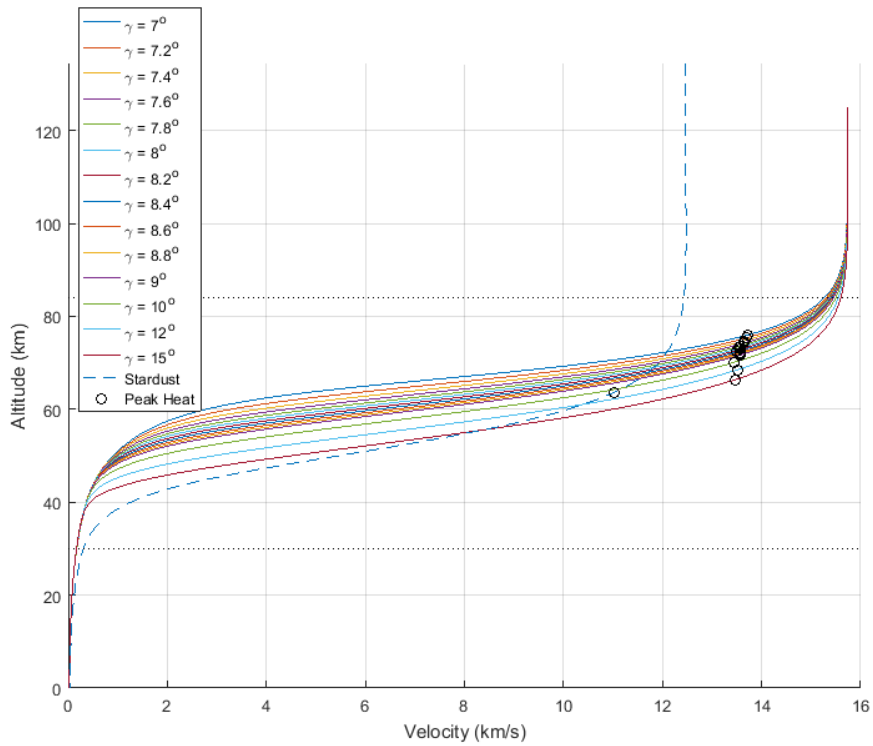
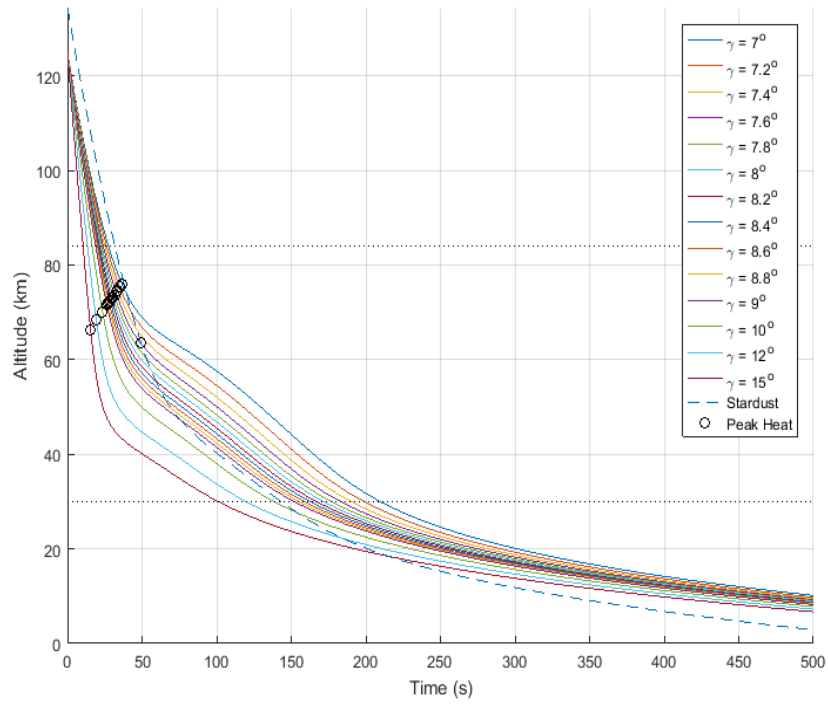
ACKNOWLEDGMENTS

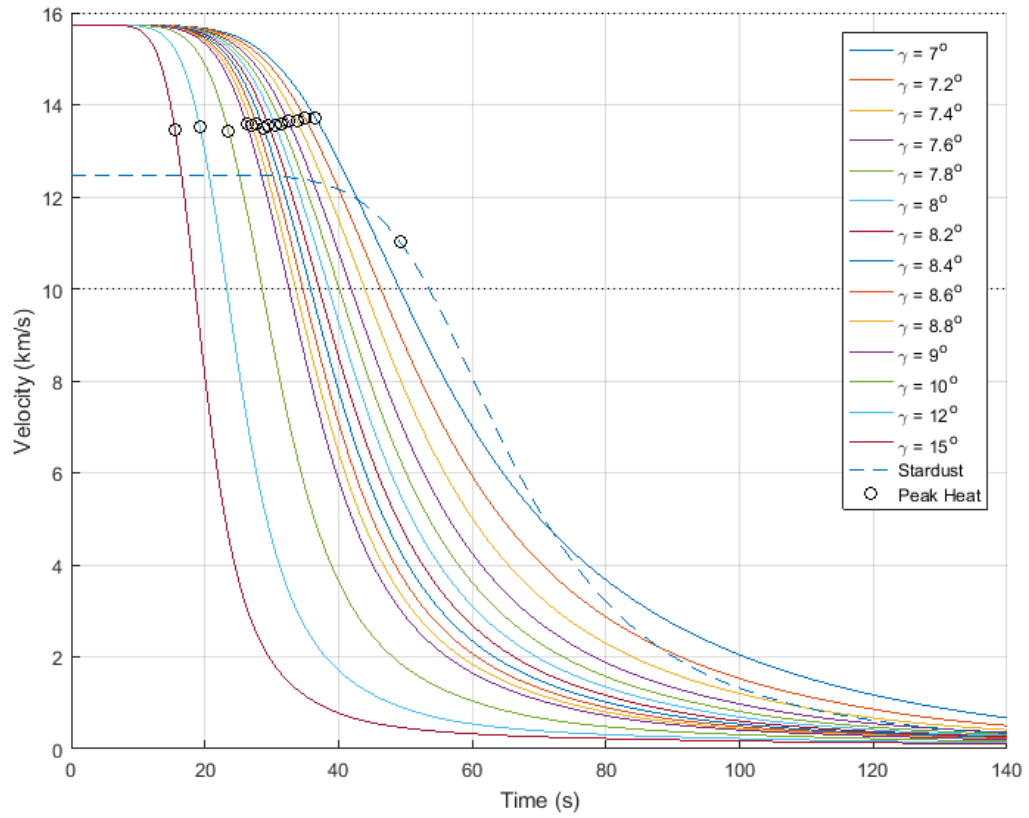
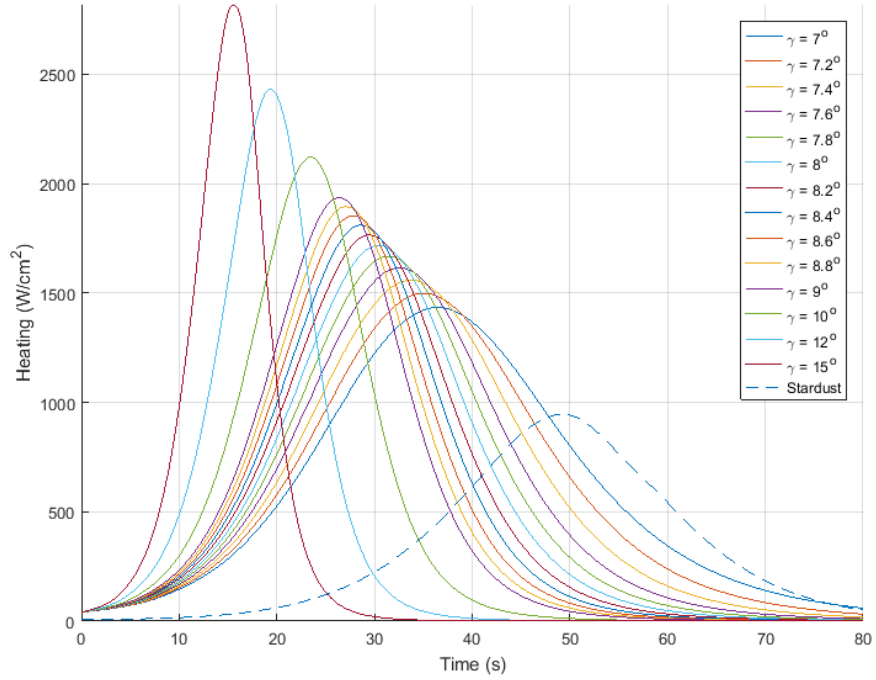
Special thanks to Jacob Brisby for his radiative heating curve fit code. Also, thanks to Prasun Desai for the more precise Stardust entry parameters. Thank you to Jerry Horsewood for giving us instruction on using the MAnE software.

APPENDIX A: AEROGEL MATERIAL PROPERTIES

Properties	Value
Density	0.1 (0.3 - 0.05) g/cm ³
Dielectric Constant	1.02 - 1.48 (@20 Ghz)
Surface Area, BET	800 m ² /g
Percent Solids	0.5 - 14%
Mean Pore Diameter	~20 nm
Primary Particle Diameter	2 - 5 nm
Index of Refraction	1.002 - 1.063
Thermal Tolerance	to 500°C
Poisson's Ratio	0.24
Young's Modulus	10-010 MPa
Tensile Strength	16 kPa
Fracture Toughness	~0.8 kPa*m ^{1/2}
Compressive Modulus	0.3 MPa
Coefficient of Thermal Expansion (CTE)	2 ppm/C° @20 - 80°C
Electrical Resistivity	10 ¹⁵ ohm-cm
Thermal Conductivity in Air	0.016 W/m/°K
Thermal Conductivity in Vacuum	0.004 W/m/°K
Sound Velocity Through the Medium	< 200 m/sec
Transparency	>90% visible wavelengths

APPENDIX B: ADDITIONAL RESULTS FOR 20CM DIAMETER





REFERENCES

- ¹ Mars Aerocapture: Extension and Refinement, Wercinski, P.F. and Lyne, J.E., *Journal of Spacecraft and Rockets*, Vol. 31, No. 4, pp. 703-705, 1994.
- ² Critical Need for a Swingby Return Option for Early Manned Mars Missions, James Evans Lyne and Lawrence W. Townsend, *Journal of Spacecraft and Rockets*, Vol. 35, No. 6, pp. 855-56, Dec. 1998.
- ³ Enceladus Mission Architecture Using Titan Aerogravity Assist for Orbital Capture About Saturn, P. Ramsey and J.E. Lyne, *Journal of Spacecraft and Rockets*, Vol. 45, No. 3, pp. 635-638, June 2008.
- ⁴ Radiative Heating of Ablating Carbon Phenolic Heat Shields, J.E. Lyne and Michael E. Tauber, *Journal of Thermophysics and Heat Transfer*, Vol. 48, No. 2, 2011.
- ⁵ Jones, D. R., "Trajectories for Flyby Sample Return at Saturn's Moons", Jet Propulsion Laboratory, California Institute of Technology, Pasadena, CA, 2016.
- ⁶ Desai, P. N., Qualls, G. D., "Stardust Entry Reconstruction", NASA Langley Research Center, Hampton, Virginia, 2008.
- ⁷ Mitcheltree, R. A., Wilmoth, R. G., Cheatwood, F. M., Brauckmann, G. J., Greene, F. A., "Aerodynamics of Stardust Sample Return Capsule", NASA Langley Research Center, Hampton, Virginia, 1997.
- ⁸ Desai, P. N., Lyons, D. T., Tooley, J., Kangas, J., "Entry, Descent, and Landing Operations Analysis for the Stardust Re-Entry Capsule", NASA Langley Research Center, Hampton, VA, 23681-2199, Jet Propulsion Laboratory, Pasadena, CA 91109-8099.
- ⁹ Ishii, N., Yamada, T., Hiraki, K., Inatani, Y., "Reentry Motion and Aerodynamics of the MUSES-C Sample Return Capsule", The Institute of Space and Astronautical Science, JAXA, Sagami-hara, Japan, Kyushu Institute of Technology, Kita-Kyushu, Japan, 2006.
- ¹⁰ Deiwert, G.S., and Marvin, J.G., "Convective heat transfer in planetary gases." *AIAA Journal*, Vol. 4, No. 4 (1966), pp. 727-728.
- ¹¹ Tauber, M E, and Sutton, K, "Stagnation Point Radiative Heating Relations for Earth and Mars," *J. Spacecraft and Rockets*, 1991
- ¹² Brisby, J., "Improved Modeling of Atmospheric Entry for Meteors with Nose Radii Between 5cm and 10m", University of Tennessee, Knoxville, TN, 2016.
- ¹³ Sutton, K. and Hartung, L. C. (1990) Equilibrium radiative heating tables for Earth entry. NASA TM 102652, May 1990
- ¹⁴ McNamara, K. M., Schneberk, D. J., Empey, D. M., Koshti, A., Pugel, D.E., Cozmuta, I., Stackpoole, M., Ruffino, N. P., Pompa, E. C., Oliveras, O., Kontinos, D. A., "X-Ray Computed Tomography Inspection Of The Stardust Heat Shield", NASA Johnson Space Center, Lawrence Livermore National Labs, Sierra Lobo, Inc., NASA Goddard Space Flight Center, Eloret Corporation, Jacobs Technology, NASA Ames Research Center.
- ¹⁵ Tran, H. K., Johnson, C.E., Rasky, D.J., Hui, F.C., Hsu, M.T., Chen, T., Chen, Y.K., Paragas, D., and Kobayashi, L., "Phenolic Impregnated Carbon Ablators (PICA) as Thermal Protection Systems for Discovery Missions," NASA TM 110440, 1997.
- ¹⁶ Witkowski, A., "The Stardust Sample Return Capsule Parachute Recovery System", Pioneer Aerospace Corporation, South Windsor, Connecticut, 1999.
- ¹⁷ Kontinos, D, Jordan, D, and Jenniskens, P, "Stardust Hypervelocity Entry Observing Campaign Support", NASA Ames, 2006
- ¹⁸ Kontinos, D. A., Stackpoole, M., "Post-Flight Analysis of the Stardust Sample Return Capsule Earth Entry", Ames Research Center, Moffett Field, California, ELORET Corp., Sunnyvale, California, 2008.